Numerical Methods for Coupled Problems
Fluid Structure Interaction

Mohammad Shahid

August 23, 2020

Fluid structure interaction is defined as the interaction between a fluid flow and a deformable body. The body can be exposed to either internal or external flow. In many engineering applications the forces from a moving fluid applied onto the boundaries of a structure will only lead to very small deformations of the structure. In these cases the structural response can be established independently after the characteristics of the fluid motion has been determined since the structural deformation does not affect the fluid flow. In those cases when the fluid forces lead to substantial deformations of the structure and the fluid flow pattern changes, the dynamics of the systems need to be coupled.

The FSI-problems are in general to complex to solve analytically so they have to be analyzed by numerical simulations. Two main approaches exist for the simulation of FSI-problems: monolithic and partitioned approach. A monolithic or direct approach is when the equations governing the flow and the displacements of the structure are solved simultaneously. The discretization of the problem leads to a large matrix of equations which is solved with a single solver. The monolithic approach has the advantages of stability since the mutual influence of the fluid and the structure can be taken into account directly. A partitioned approach is when the equations governing the flow and the displacement of the structure are solved separately with two distinct solvers. This will allow for codes specialized for flow equations and structural equations and hence possibly more efficient solution techniques for each of them. On the other hand; the partitioned approach requires a coupling algorithm to allow for the interaction and to determine the solution of the coupled problem.

Partitioned algorithms use subsequent solutions of the fluid and structure sub-problems and the interaction is either loosely or strongly coupled. A loosely coupled algorithm is explicit and the codes will have only one bidirectional exchange of solved variables per time step, in a sequentially staggered manner. A strongly coupled algorithm (implicit) uses an iterative staggered scheme which performs sub-iterations over the single fields to converge at the end of the time-step.

1 Exercise 1

In this exercise a case corresponding to an imposed motion in the X-direction for a NACA0012 profile was run where only an X-motion is imposed using a classical ramp. The evolution of the forces F_X and F_Y at time $t = 0$ to when the target velocity is reached are examined. Figure 1 shows the evolution of forces F_X and F_Y with time.

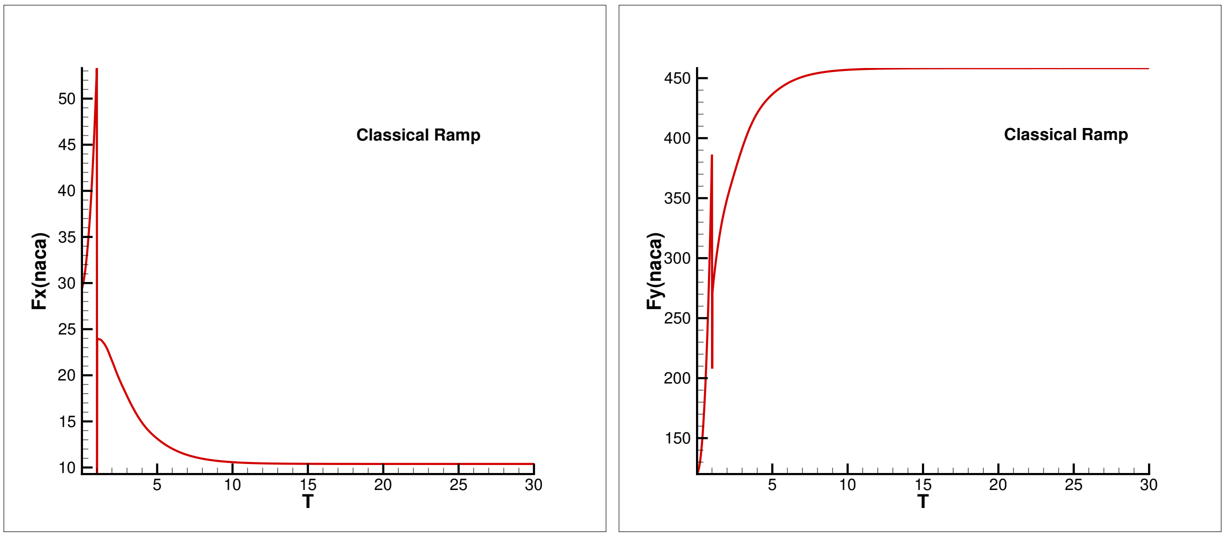

Figure 1: Evolution of Forces with time

From figure 1 it is evident that the force is not zero at time $t = 0$, this behaviour is attributed to the added mass effect. There is a sudden change in the value of forces because even when the acceleration of the body is zero, the flow needs some time to stabilize due to the effect of added mass.

To evaluate the added mass coefficient another simulation is performed with T_X and T_Y solved motion with only one time-step. The estimation mode of the of the added mass coefficient, i.e. the added mass divided by the mass of the body, is switched to an accurate evaluation with frequency=0 which means that the added mass coefficient is only computed at the beginning of the computation. Another similar case but with approximate computation was also performed to compare the results of the two modes of computation. In accurate mode, a loop is carried out to converge all the explicit terms which appear in the discretization of the gradient while in approximate mode the terms are not resolved which improves the computation time significantly with much compromising on the results. The evaluated added mass coefficients for all the cases performed till now has been tabulated in Table 1.

Cases	M_{xx}	M_{xy}	M_{yx}
T_X imposed & T_Y fixed	2.91×10^1	1.15×10^2	1.12×10^2
T_X & T_Y solved (accurate)	2.95×10^1	1.20×10^2	1.20×10^2
T_X & T_Y solved (approximate)	2.95×10^1	1.20×10^2	1.20×10^2

Table 1: Added mass coefficient for different cases

From table 1 we can clearly see that the order of magnitude of M_{xy} and M_{yx} are equal in both computation modes. Hence an improvement in the computation time can be achieved by using the approximate mode since the accurate mode resolves all the explicit terms in the computation of the gradient which requires a significant amount of computation time.

2 Imposed motion in X-direction with action of Linear Spring in Y-direction

In this case from the first computation with an imposed motion in X-direction, a new computation is defined with the DOF T_Y as solved including the action of a linear vertical spring. To impose the force generated by the spring a spring stiffness is chosen to have a displacement of magnitude equal to 1/4 of the chord which comes to be 1833.2 N/m. The position of the spring and the centre of mass does not matter here since only one DOF of translation is involved. Two cases were studied using the action of linear vertical spring:

2.1 Case 1: Solid density is equal to 10 times the fluid density

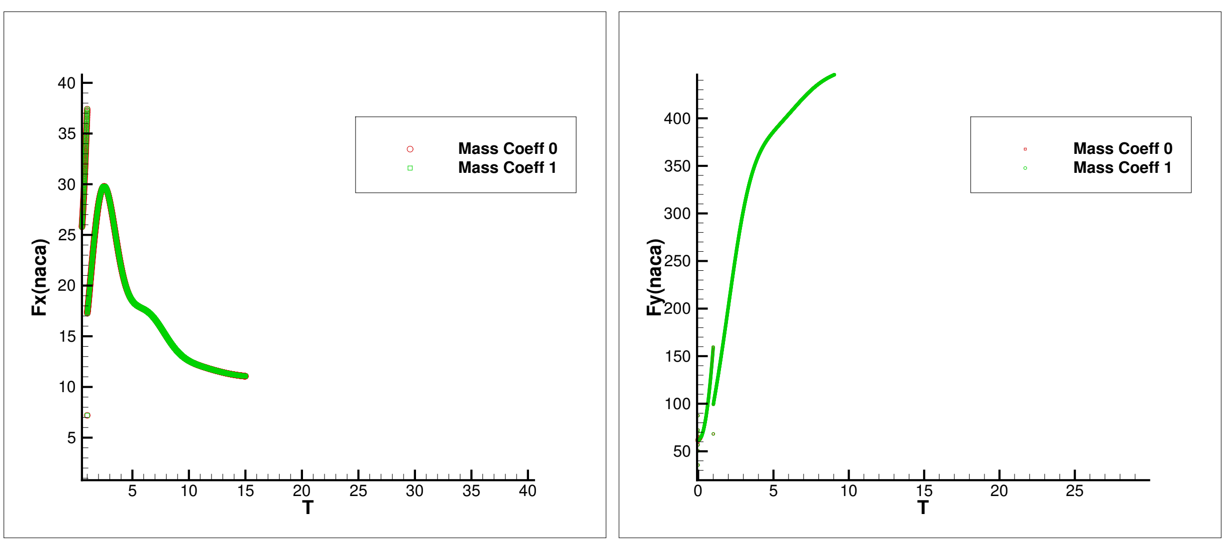

Figure 2: Evolution of Forces with time for different mass coefficients

Since the volume of the profile per unit width is given as $0.08\, m^3/m$ and the fluid density is $1000\, kg/m^3$, the mass of the body was taken as $800\, kg/m$. We utilized the Adaptive

grid refinement technique in which the solution is evaluated using the rigid body motion or weighted mesh deformation. In adaptive grid refinement technique the mesh is updated in each iteration loop. Two set of sub cases were performed using the added mass coefficient as 1 and 0 in the next, for the weighted deformation of the DOF T_Y.
It is evident from figure 2 that the added mass coefficient has no influence on the evolution of forces as the mass of the body is quite high as compared to the liquid, hence the added mass effect is negligible.

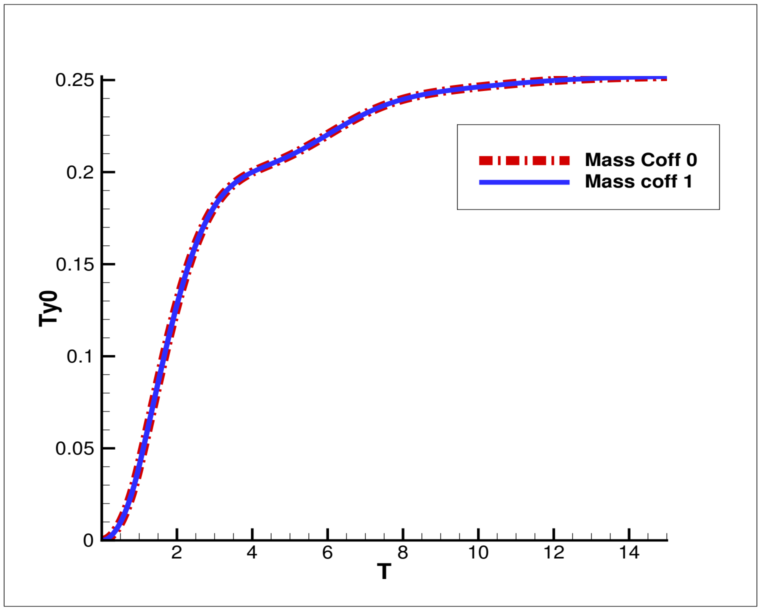

Figure 3: Position vs time for the body

Since we have taken the force constant of the spring for 0.25 m vertical displacement. The final position we got from the solution comes out to be what we expected (Figure 3).

2.2 Case 2: Solid density is equal to the fluid density

In this case the mass of the body was taken as $80\,kg/m$. Now since the mass of the body is quite less hence the effect added mass will be more pronounced which will result in the stability issues for the coupling. A wide variety of stability issues regarding FSI-problems and partitioned algorithms have been reported. Most of the problems are in regard to the loosely coupled algorithm.

When using a loosely coupled algorithm to solve FSI-problems with incompressible flow and slender structures, it has been observed that instabilities in the computations will occur. The instabilities depend on the mass density of the fluid versus the mass density of the structure, but also the geometry of the domain has importance. It has further been observed that decreasing the time step size will result in even more instability, or that the instability occurs earlier. The instability is inherent in the scheme itself and has been named “artificial added mass effect”. The name comes from that the fluid closest to the coupling interface will act as extra mass on the structure, increasing its inertia. In sequentially staggered schemes the fluid forces depend on predictions of the interface displacement instead of the actual ones. Errors in the prediction together with the added mass effect will lead to incorrect coupling forces which yields the instability.

It has been observed that loosely coupled algorithms are unstable for low density ratios and the instabilities increase as the ratio gets lower. Also, strong coupled algorithms are affected by the density ratio in such a way that an increased number of iterations are needed within each time-step in order to achieve convergence of forces along the interface at the end of the time-step. Hence to stabilize the coupling the added mass coefficient parameter was set to 1 (User Defined). Two other simulations were performed with accurate and approximate mode of computations and the evolution of forces with time are analyzed.

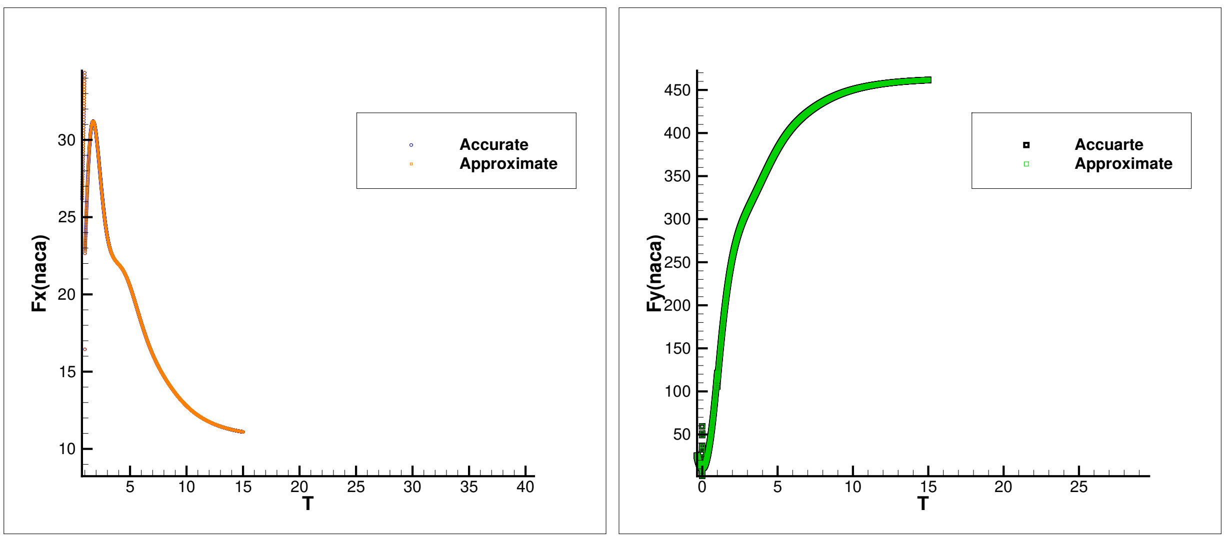

Figure 4: Evolution of Forces Fx and Fy with time for accurate and approximate evaluation of added mass coefficient

From figure 4, it is evident that using either approximate or user defined added mass coefficient has the same effect as that of the accurate mode. Hence any one of them can be chosen to solve the problem.

3 Suddenly imposed vertical acceleration

In this case a sudden vertical acceleration is imposed on the airfoil i.e. T_y imposed and T_x fixed, and the the added mass coefficients are compared with analytical results by considering the airfoil as a flat plate.

For a flat plate added mass can be evaluated analytically as:

$$m_a = \rho \pi a^2$$

where is the half chord length of the airfoil which is equal to 1/2 in our case. Using the above expression the added mass m_a comes out to be 785.4 kg/m and since the mass of the body is 80 kg/m. Hence the added mass coefficient can be calculated by taking the ratio of the added mass to the mass of the body.

Added mass coefficient $= m_a/m = 9.81$

From the simulation we find that the difference between the force values is around 755 N. Hence the added mass can be calculated as the ratio between the difference between the force and the sudden change in acceleration, which comes out to be 755 kg/m.

Added mass coefficient $= M_{yy}/m = 9.43$

It can be concluded that the order of magnitude of the added mass coefficient calculated using the simulated results is similar to those computed using the analytical expression for a flat plate.

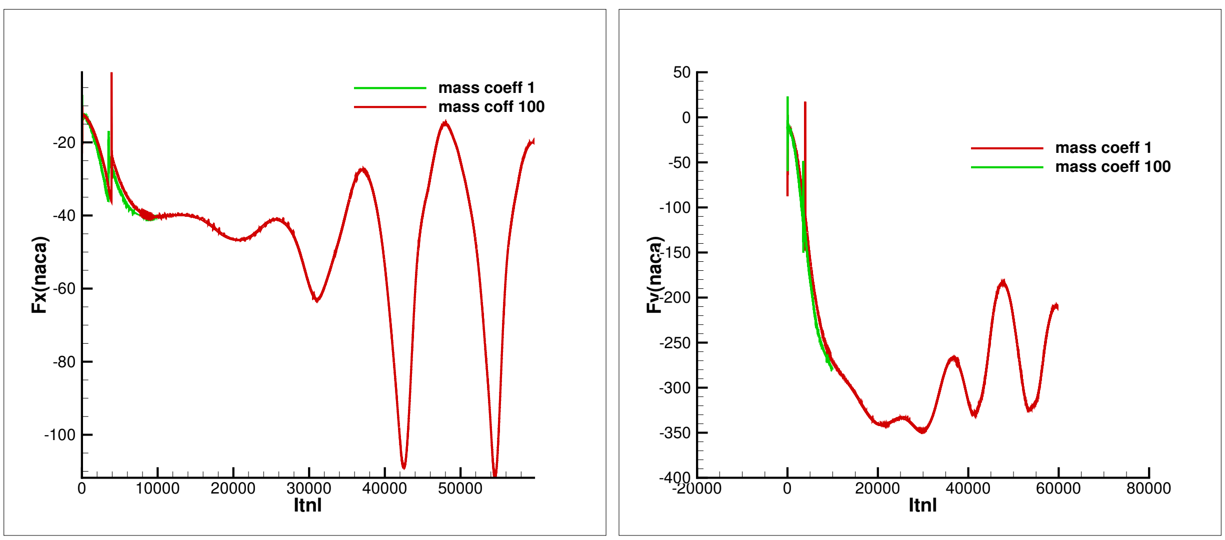

Figure 5: Evolution of Forces with iterations

Now if we impose a very large value of added mass coefficient, 100 in our case, it can be seen from figure 5 that the force F_x does not converge at each non-linear iteration as the added mass matrix is over relaxed causing the problem.

4 Frequency of oscillation of airfoil when released with initial vertical displacement in a fluid at rest

In this case the frequency of oscillation of the airfoil is calculated when it is released in a fluid at rest. In order to do that we defined a new computation with only T_Y as solved keeping

T_X fixed. The initial translation T_{y0} is set to 0.25 and the frequency obtained is compared with the natural frequency of the mechanical system.

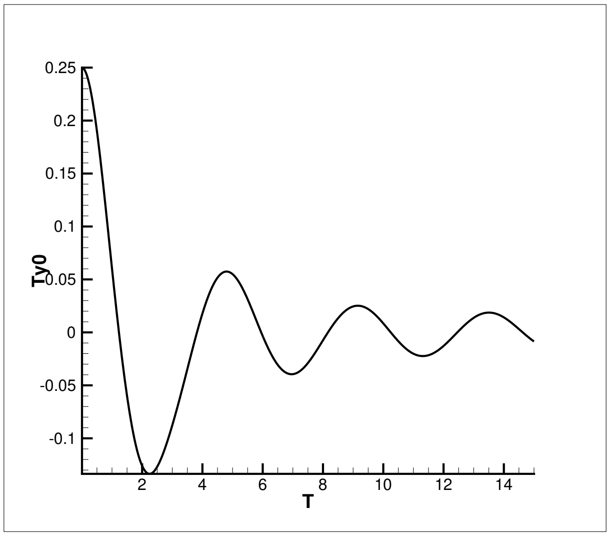

Figure 6: Displacement vs Time plot for the airfoil

Frequency of the mechanical system is given by:

$$f = \frac{1}{2}\sqrt{\frac{k}{m}}$$

which comes out to be 0.76 Hz. Figure 6 shows the variation of displacement of the body with time. From figure 6 we can calculate that the time period of oscillation of the body is around 4.2 seconds, hence the frequency comes out to be 0.24 Hz, which is less than the natural frequency. It is due to the added mass effect, as the total mass of the system would increase and since the frequency is inversely proportional to the mass of the body, the frequency will decrease. The evolution of the displacement with time corresponds to the damped oscillation case.

Study of 2D breaking dam on Elastic Wall

In this part of project numerical investigations are carried out to demonstrate the fluid structure interaction with free surfaces in the case of collapse of a water column onto a wall for rigid and elastic ones and the numerical results obtained are then discussed and compared. Simulations are also carried out to study the influence of grid, time step and number of modes on the displacement of the tip and on the forces concerned. For this well-known example, our first goal is to reproduce the test-case 4.2 of the article Walhorn (2005). In this configuration a water column of width 0.146m is placed in the left corner of a tank of height 0.584m. Free surface location of water is kept at 0.292m. The tank is open at the top and at the bottom wall and a rectangular obstacle (width = 0.024m and height = 0.084m) is fixed in the middle. As far as the boundary conditions are concerned, slip boundary conditions are imposed at the walls and constant pressure is prescribed at the top. The fluid properties correspond to water and air taken are: For water, density = 1000 kg/m3 while for air, density = 1kg/m3.

5 Study of unsteady analysis of 2D-breaking dam on obstacle

In this exercise in order to get insight of the fluid-structure interaction with free surfaces, numerical simulations are carried out for two cases, one for rigid wall obstacle and other for elastic wall in the subsequent sections. .Numerical details for these simulations on the fine marine are as follows: We have selected unsteady analysis to figure out the advancing front of free surface, an Euler equations to solve flow model, Initial conditions: Initially water is assumed to be at rest. Boundary conditions: For top boundary, we have prescribed pressure and for other boundaries slip boundary condition for in-viscid flow is considered.An adaptive time step based on Courant Number 0.3 is used here for defining time step .Here we make use of the adaptive grid refinement using a Free surface tensor criterion,which refines the cells anisotropically when the free surface is aligned to the cells.

5.1 Rigid wall

Here keeping all the parameters as stated above are same the simulations are carried out using the volume of fluid method and finite volume schemes using mesh points of 40X30.

5.2 Results and Discussion

The results for the advancing front (Fig. 7) in presence of the rigid obstacle are compare to the one for case 4.2 of Walhorn (2005). As it can be seen from the snaps of advancement of free surface with time recorded at various time interval, that initially, the water column collapses under gravity after that when this thin front has passed the rigid wall and reaches the right wall of the tank, it encloses a region of air thus develop second front close to the top of the obstacle and finally the bridge-like water structure collapses.

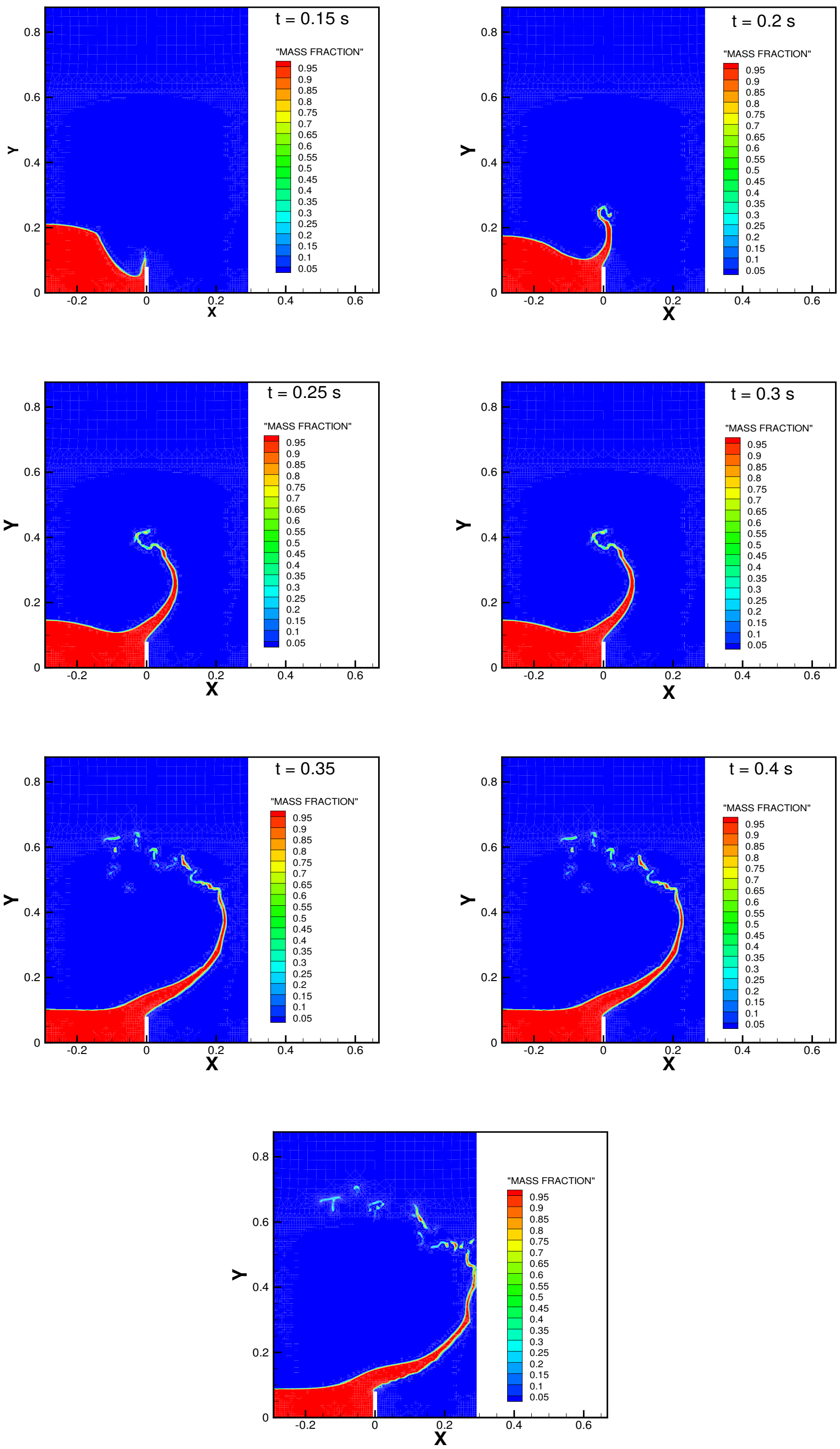

Figure 7: Time history of collapsing of water column with rigid wall

5.3 Flexible wall

Here keeping all the parameters same the simulations are carried out on the mesh points using modal approach with the number of modes of vibrations used are 3.In this approach a structural solver by modal synthesis is already integrated inside the flow solver. This approach exploit the natural frequencies and the mode shape of the structure, to computes the solid body deformation under the action of fluid loads. These natural frequencies and the mode shapes are determined outside the flow solver and prior to any CFD computation,using a modal analysis with ABAQUS.

5.4 Displacement of Upper left corner of flexible wall tip

Figure 8 shows the displacement of the time history of the upper left corner of flexible wall tip for time equal to 0.75 s and the corresponding mesh of the domain used at an instant of t=0.25 s for the simulation. It can be seen that the mesh is not well adapted to the free surface and even the near wall of the flexible wall tip is not well refined which needs to be taken in to consideration in order to accurately capture the flow physics of the free surface.

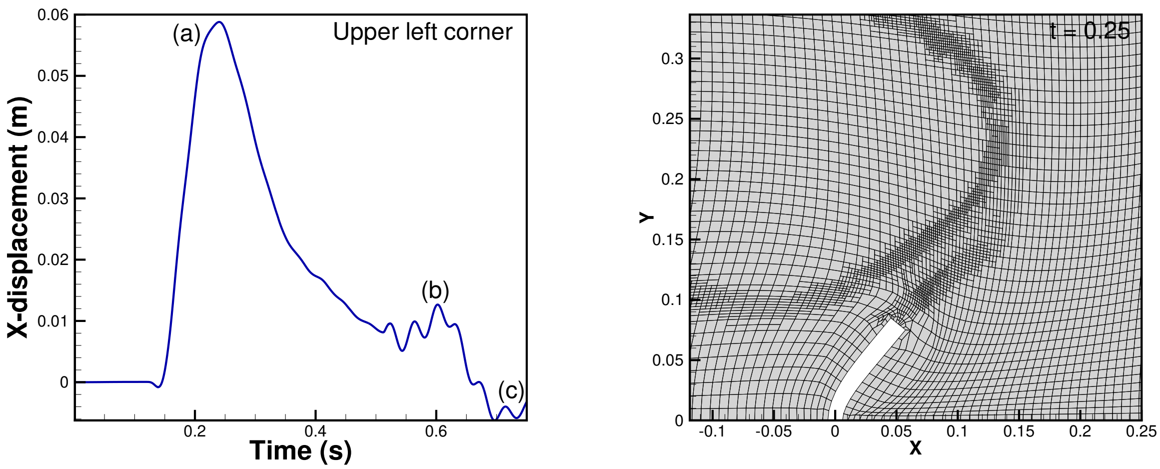

Figure 8: History of displacement left and snapshot of impact of water front for maximum displacement

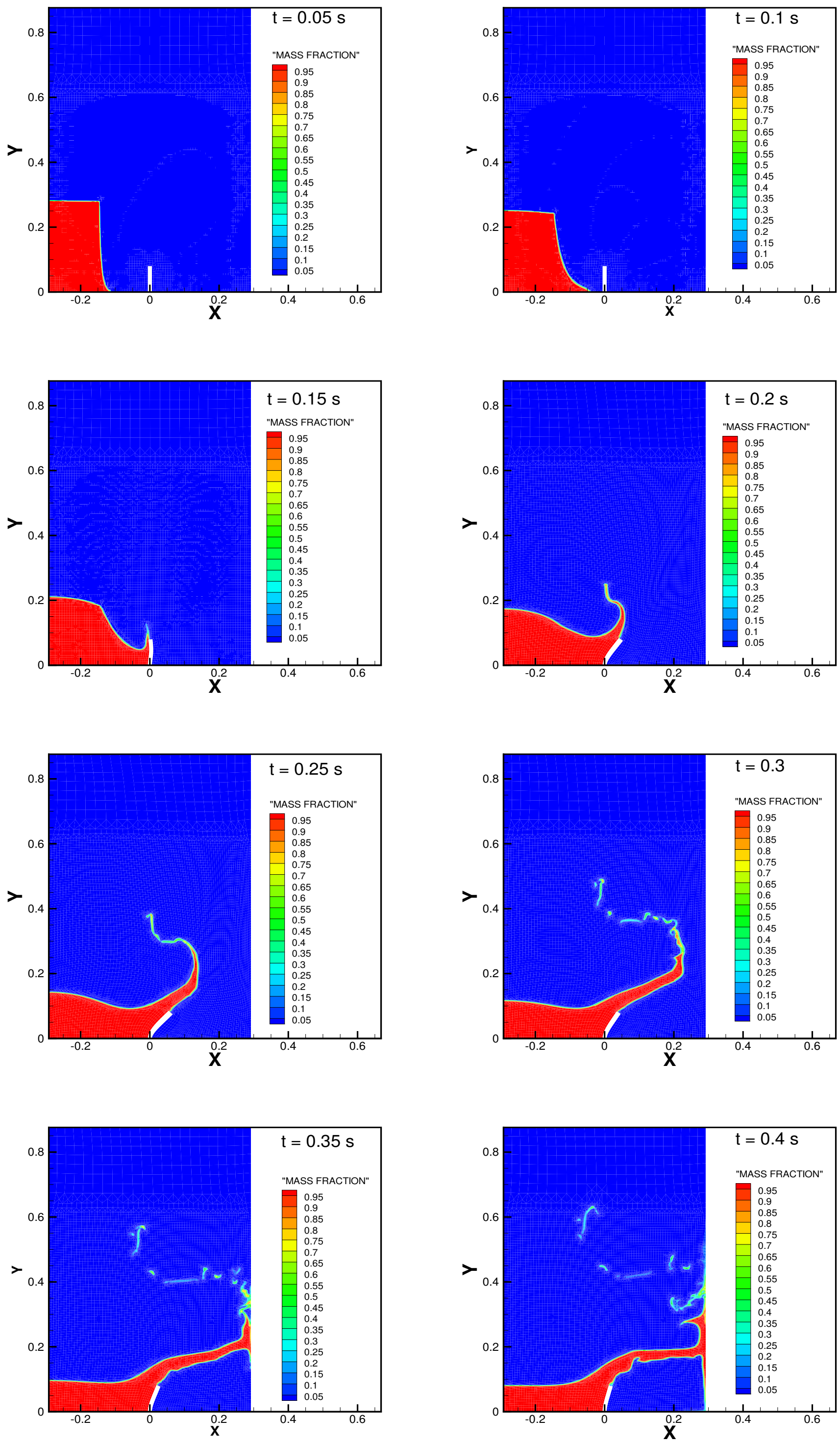

Figure 9: Time history of collapsing of water column with flexible wall

5.5 Results and Discussions

The time marching solution of advancing front (Fig.9) in presence of the elastic wall are again compare and is found to be in good agreement with the Walhorn (2005) for the test case 4.2. As compare with the rigid wall, the water column shows similar behavior until the water front strikes the elastic wall,as shown in (Fig. 9). This water front then strikes impulsively with the elastic wall. The elastic structure is then deformed by the impulse of the fluid wave (Fig.wall.). The deformation of the elastic wall to the right make the way to the to rises. The maximum deflection for the elastic wall is reported at the upper left corner of the obstacle (in (a) Fig.9) when the water jet passes the top and is fully attached to the left side of the structure. Finally, the impact of the fluid causes the thin structure to start oscillating (b). This oscillation is damped (c) by the water located left and right of the wall.

5.6 Comparison of forces obtained from rigid and elastic structures

In this section the results obtained from the above simulations for rigid and elastic structures are compared and analyzed. It is evident from the Figure 10 that initially the horizontal force on the plate for both rigid and elastic wall is zero until it strikes the structure. As soon as the water front impinges on the structure, the force on both the structure rises and attains maximum value and then decreases with time. The maximum magnitude of force at the moment when water front strikes the structure is greater in case of rigid wall because it resist all the impacts of water front while elastic wall doesn't sustain the impacts and started deforming as soon as the water front impacts on it thus unable to resist all the impacts put upon it.

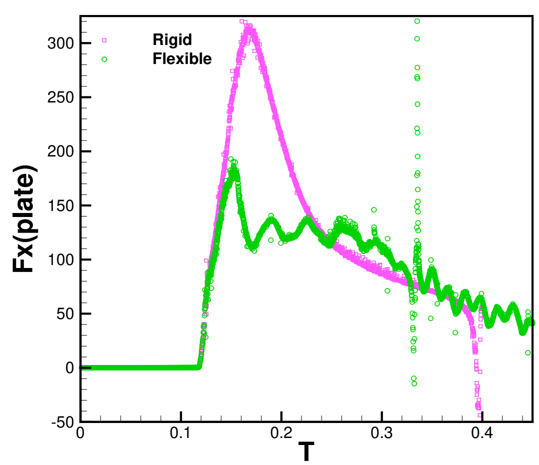

Figure 10: Comparison of horizontal force with time for rigid and flexible wall

6 Influence of the numerical parameters on the displacement of the tip and the forces.

In the subsequent section the influence of the numerical parameters like the grid size, time step and number of modes on the displacement of the tip and and the forces are studied on the elastic wall using modal approach.

6.1 Influence of grid size.

In this section in order to study the effect of grid size we have selected two grids G1(20X30) and G2(40X50) while all the parameters are kept constant as discussed above. The results obtained are then compared and discussed in regard with the displacement of the tip, the residual and the force on the wall.

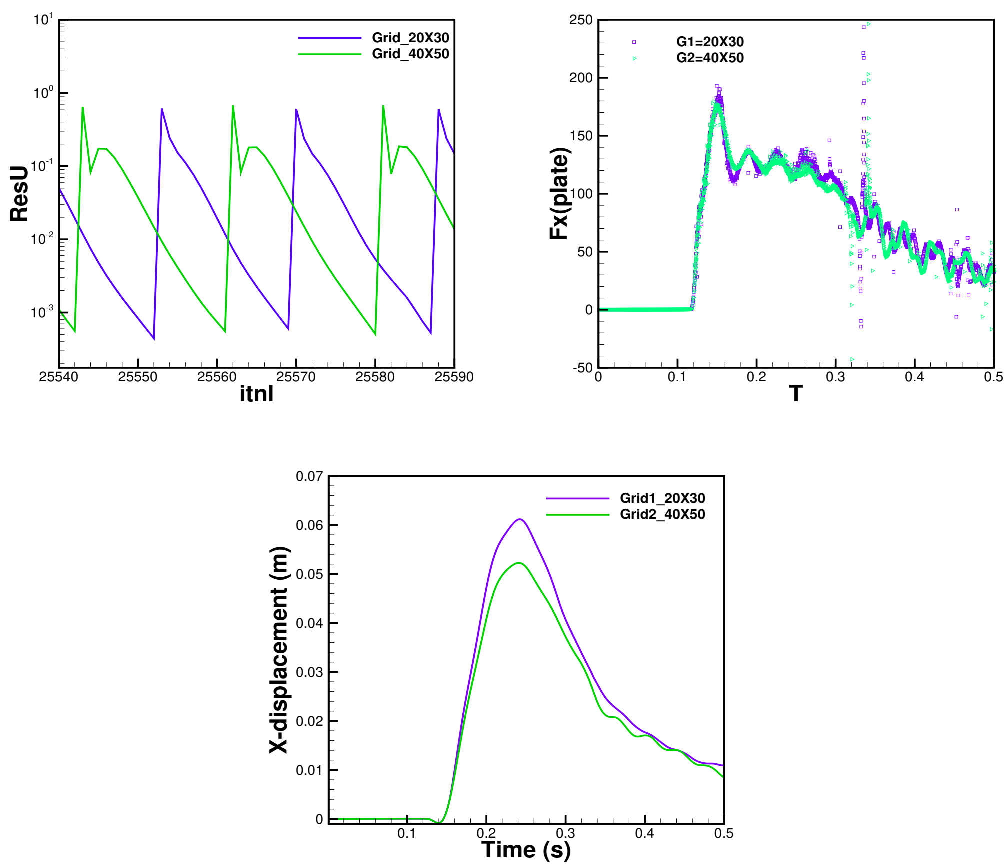

Figure 11: Influence of grid size on ResU(top left), Horizontal force,Fx(Top right) and Displacement of tip(bottom)

From Figure 11 of the ResU versus non-linear iteration, horizontal force F_x versus time, and X-displacement versus time we can observe that as the grid is refined it takes more iterations to resolve the variables. However, evolution of the horizontal force with time is quite similar in both the cases. There is a small over estimation of the horizontal displacement in case of the coarser grid at around 0.25s but after that the profiles in both the cases converge to the same value. There are however small undulations or wiggles in case of the finer grid, this may be attributed to the larger time-step.

6.2 Influence of time step through Courant number

In this section in order to analyze the effect of time step through CFL we have selected two CFL conditions CFL(0.3) and CFL(1.0) on a grid size of 30X40, while all the parameters are kept constant as discussed above. The results obtained are then compared and discussed in regard with the displacement of the tip, the ResU and the force on the wall.

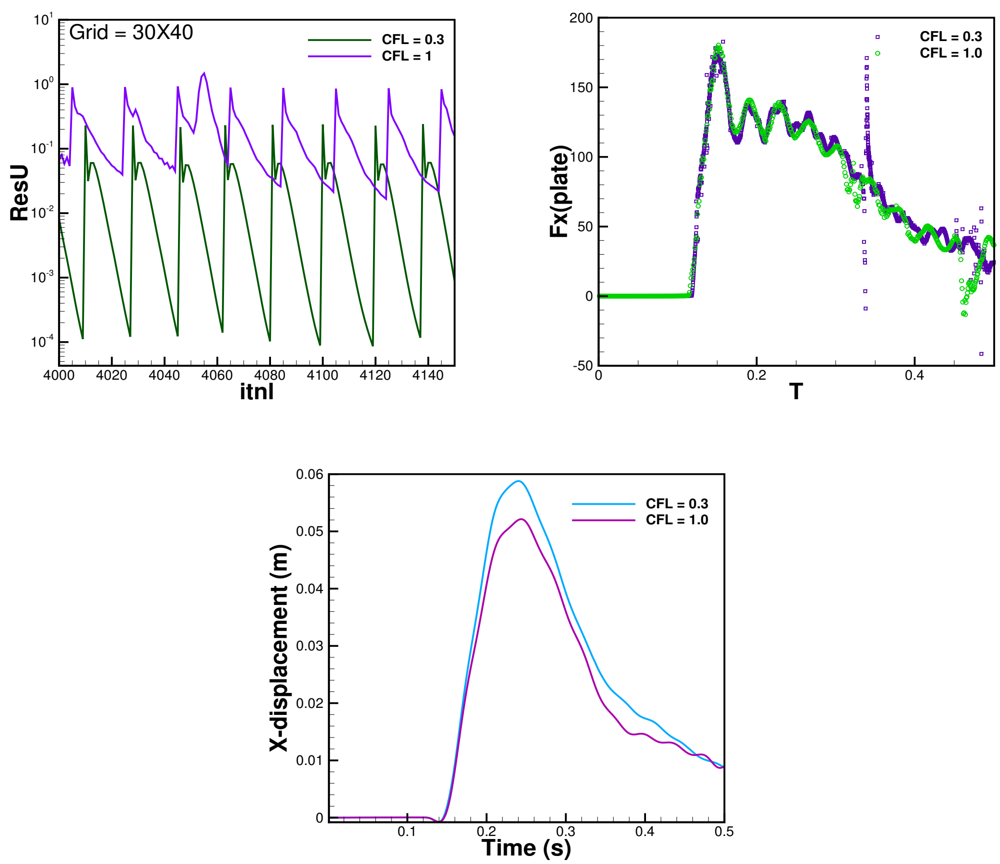

Figure 12: Influence of time step through Courant number on ResU(top left), Horizontal force, Fx(Top right) and Displacement of tip(bottom)

Figure 12 shows the influence of Courant number on the residuals of the different quantities. Changing the Courant number from 1 to 0.3 results in the decrease of the mean residuals of horizontal velocity while the evolution of the horizontal force and displacement is quite similar, the one with lower Courant number (i.e. lower time-step) being smoother as compared to the other.

6.3 Influence of number of modes shape

In this section in order to analyze the effect of mode shapes we have selected three sets of mode of vibrations m1(3), m2(4) and m3(6) and the simulations are carried out on Grid of 30X40, while all the parameters are kept constant as discussed above. The results obtained are then compared and discussed in regard with the displacement of the tip and the force on the wall. It can be seen from the Figure 13 of force and displacement curve with time, that increasing the number of modes from 4 to 6 does not effect more on the computations but rather it increases the computation time and hence computation cost.

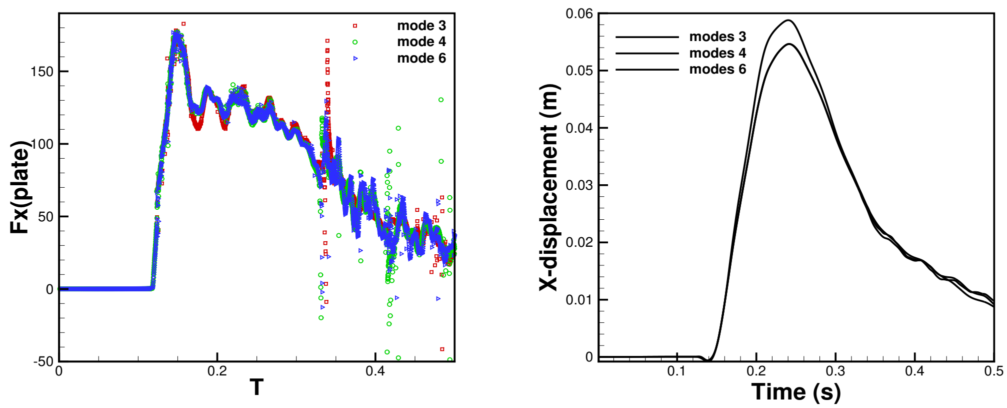

Figure 13: Influence of number of modes on Horizontal force, Fx (Left) and Displacement of tip (Right)